08,04,16

Change of the structure of dielectric spectra of vanadium dioxide films in case of chromium doping

© A.V. Ilinskyi[1], R.A. Castro[2], V.A. Klimov[1], A.A. Kononov[2], E.B. Shadrin[1]

[1] Ioffe Institute,
St. Petersburg, Russia
[2] Herzen Russian State Pedagogical University,
St. Petersburg, Russia

E-mail: shadr.solid@mail.ioffe.ru

Received March 7, 2025
Revised March 9, 2025
Accepted March 10, 2025

It is shown that increasing the degree of chromium doping of thin VO_2 films leads to a decrease in the frequencies of their dielectric spectra features and to an increase in the temperature of the semiconductor-metal phase transition. Based on the Debye formula, the parameters of the dielectric spectra are calculated using the Gavrilyak-Negami function. Macroscopic and microscopic analysis of the formation mechanism of experimental dielectric spectra features was carried out. The role of Cr-Cr-dimers of increased strength in the formation of spectra of heavily doped VO_2:Cr film was revealed.

Keywords: VO_2 thin films, dielectric spectra.

DOI: 10.61011/PSS.2025.04.61275.48-25

1. Introduction

This paper is devoted to the study of the dielectric response mechanism of VO_2 films to exposure in the frequency range of 1 Hz–10 MHz to an external sinusoidal electric field. This is an application of dielectric spectroscopy methods to the study of thin films of both pure vanadium dioxide and films doped with such a transition metal, as Cr.

Since in dielectric spectroscopy the experimentally measured quantities are the frequency dependences of the bias current $I(f)$ and the angle $\psi(f)$ between the voltage and current vectors, then for an ideal dielectric the angle ψ is frequency independent and equal to $\psi = \pi/2$ at all frequencies used in dielectric spectroscopy (10^{-3}–10^{8} Hz). It follows that for each frequency of the probing voltage oscillation, the bias current oscillation is ahead in phase of the voltage oscillation by 90°. At the same time, for a non-ideal dielectric, the angle $\psi(f)$ depends on frequency and is found to be smaller 90° by the amount $d(f) = \pi/2 - \psi(f)$. In practice, the dimensionless value $\mathrm{tg}\,\delta(f)$, which is equal to the ratio of the charge carrier drift current vector to the bias current vector, is used in analyzing experimental dielectric spectra (DS). Since the drift current is accompanied by energy losses, the value $\mathrm{tg}\,\delta(f)$ is commonly referred to as the tangent of the angle of dielectric losses.

Modern dielectric spectroscopy utilizes industrial dielectric spectrometers with high sensitivity that have computers with a variety of software. Based on the measured values $I(f)$ and $\mathrm{tg}\,\delta(f)$, the following are calculated using the programs used in the spectrometers: frequency dependences of the complex impedance $z^*(f)$, complex dielectric permittivity $\varepsilon^*(f)$, electrical capacitance of the sample cell, etc. The obtained spectra admit their rearrangement by excluding frequency f as a parameter, which makes it possible to obtain, for example, the dependence of the imaginary part of the dielectric permittivity ε'' on its real part ε', viz.i.e., the function $\varepsilon''(\varepsilon')$, positioned in the literature as the Cole-Cole diagram. Such a function, although it contains no new information, makes some singularities of the registered DS more visualizable.

Vanadium dioxide is known [1,2,3] to exhibit a semiconductor-metal phase transition (PT) at a temperature of 67 °C. A structural PT takes place in it when it is cooled below 67 °C, and the elastic stresses accompanying such a transition lead to the destruction of macroscopic crystalline samples of VO_2. At the same time, vanadium dioxide thin films do not have this „disadvantage“, which makes VO_2 films relevant for designing of various applied devices based on them, and doping changes the characteristics of the PT, allowing to select the parameters of this transition for solving specific technical problems. Experimental data obtained by the dielectric spectroscopy method make it possible to predict with high accuracy the behavior of various kinds of physical quantity sensors [4], high-speed information storage and processing systems [5], as well as femtosecond devices for protection of wide-range optical image receiving matrices [6] in the applied devices.

2. Experimental procedure

80 nm thick VO_2:Cr nanocrystalline films were synthesized on 40 μ thick optical mica substrates. The synthesis process was carried out by laser ablation [7]. Vanadium dioxide polycrystalline thin films of $V_{1-\gamma}Cr_\gamma O_2$

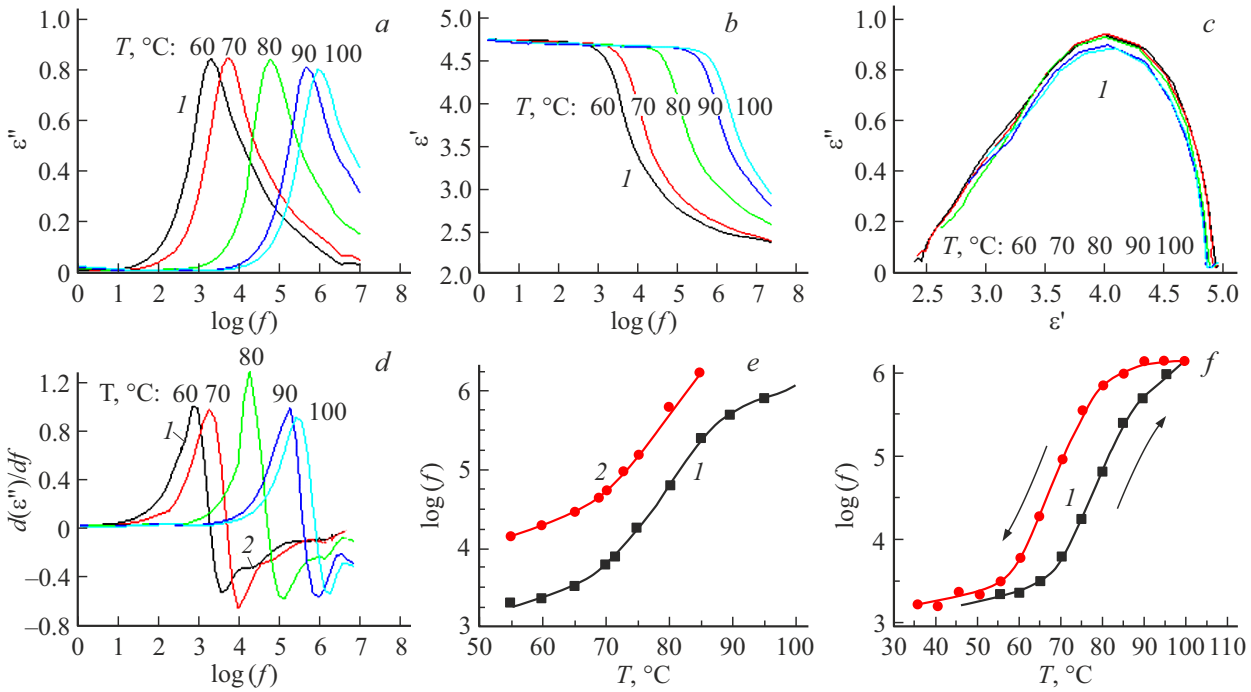

Figure 1. Sample of VO_2:Cr(1 %). The frequency dependences of the imaginary ε'' (a) and the real ε' (b) parts of the dielectric permittivity, and the CC diagrams $\varepsilon''(\varepsilon')$ (c) for different temperatures in the interval of 60–100 °C. The frequency and temperature dependences of the frequency derivative of the singularities of the imaginary part $\varepsilon''(f)$ of the dielectric permittivity (d) are also presented and, in addition, the temperature dependences of the frequency positions of the main maximum 1 and the weak maximum 2 (e) are shown. Figure 1, f shows the temperature hysteresis loop of the frequency position $f_{\max 1}(T)$ dominating the spectrum of the maximum 1.

were synthesized by simultaneous laser sputtering from metallic V (99.9 %) and metallic Cr (99.9 %) in an oxygen atmosphere at 750–900 K. The degree of doping (γ) was judged from the relative evaporation time of each target. The article presents measurement results obtained for both weakly doped VO_2 and heavily chromium-doped films (1 at.%, 3 at.%).

„Concept-81“ spectrometer was used for dielectric measurements. The studied film was placed in a spectrometer cell fabricated as a planar capacitor. The capacitance of the empty cell $C_0 = \varepsilon_0 S/d$ (S is the electrode area, d is the mica thickness) was 27 pf. The measurements were performed in the frequency range of $f = 10^{-1}$–10^7 Hz. DS were studied over the range of 55–100 °C at fixed temperatures that were changed with a step of 5 °C.

The frequency dependences of the real $\varepsilon'(f)$ and imaginary $\varepsilon''(f)$ parts of the complex dielectric permittivity ε^* of the sample are covered separately in this paper. The experimental results of $\varepsilon'(f)$ and $\varepsilon''(f)$ were also reconstructed as Cole-Cole diagrams for the convenience of DS analysis: $\varepsilon''(\varepsilon')$.

3. Experimental results

3.1. Sample VO_2:Cr(1 %)

Figure 1, a shows the frequency dependences of the imaginary $\varepsilon''(f)$ part of the dielectric permittivity of a film sample of vanadium dioxide weakly doped with chromium (VO_2:Cr(1 %)) obtained at different temperatures. A single maximum (№ 1) located in the frequency region $f = 10^2$–10^6 Hz is clearly observed on these dependencies. The value of the function $\varepsilon''(f)$ at the maximum is $\varepsilon''(f_{\max}) = 0.85$. The maximum shifts toward higher frequencies as the temperature increases. The frequency position of the maximum of the function $\varepsilon''(f)$ abruptly shifts toward high frequencies from 1.3 kHz to 1 MHz as the temperature rises from 60 to 75 °C, and the numerical value of its magnitude does not change much with the frequency change.

Figure 1, b shows the frequency dependences of the real $\varepsilon'(f)$ part of the dielectric permittivity of the film sample VO_2:Cr(1 %). Here one step of the functional dependence $\varepsilon'(f)$ is clearly observed and the middle of this dependence is at the frequency $f_{\max} = 1.3$ kHz at $T = 60$ °C. The frequency at which the step function $\varepsilon'(f)$ is located monotonically increases without abrupt changes from 1.3 kHz to 10 kHz as the temperature increases in the range of 60–65 °C. However, the midpoint of the step is accelerated toward high frequencies and at 100 °C is located already at 1 MHz in the temperature range of 65–80 °C (curves *4, 6* of Figure 1, b). As the temperature decreases, the DS singularities shown in Figure 1, a and b return to their original position on the frequency scale, but with a temperature lag of 10 °C relative to their position at heating.

It is possible to follow the temperature transformation of the DS of VO_2:Cr(1 %) sample more definitely and with

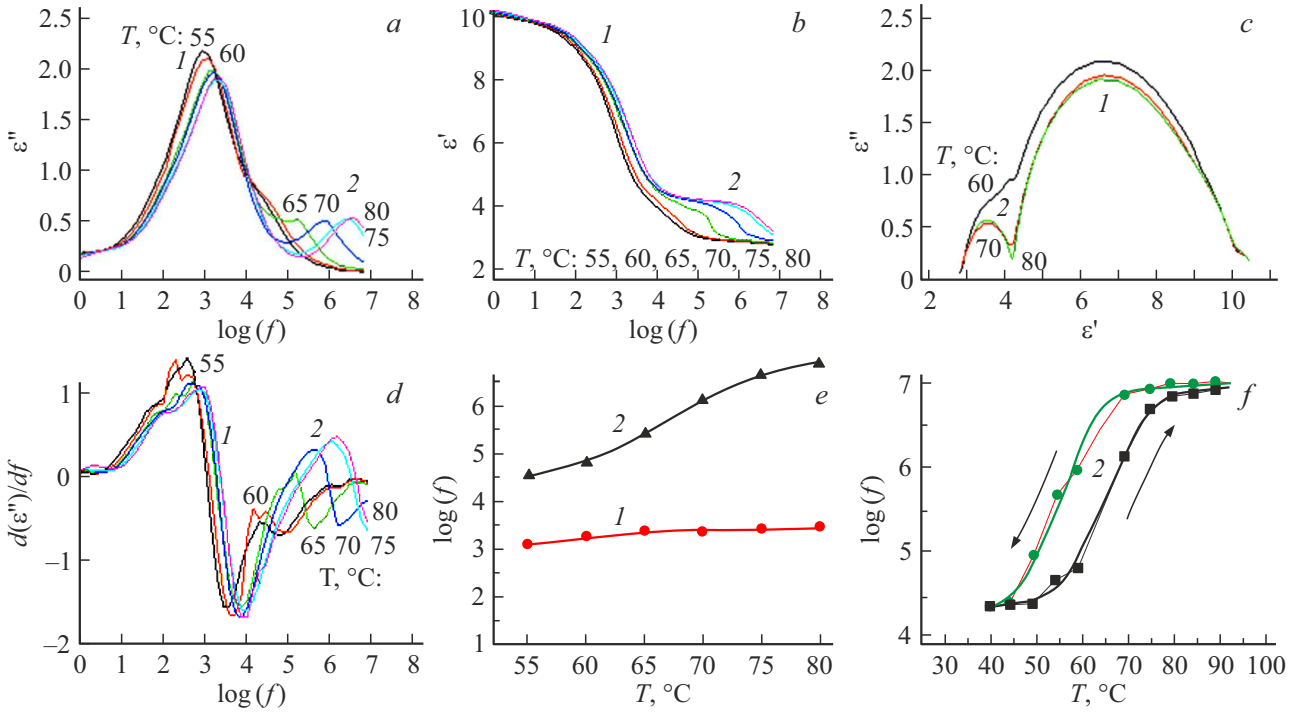

Figure 2. VO_2:Cr(3 %) sample. The frequency dependences of the imaginary ε'' (*a*) and real ε' (*b*) parts of the dielectric permittivity, as well as the CC diagrams $\varepsilon''(\varepsilon')$ (*c*) for temperatures in the range of 55–80 °C. In addition, the frequency and temperature dependences of the frequency derivative of the features of the imaginary part ε'' (*f*) of the dielectric permittivity (*d*) and the temperature dependences of the frequency position of the main maximum № 1 as well as of the weakly expressed maximum № 2 (*e*) are presented. The temperature hysteresis loop of the frequency position $f_{\max 2}(T)$ of the maximum № 2 is shown in Figure 2,*f*.

greater accuracy by differentiating by frequency f of the function $\varepsilon''(f)$. The result of differentiating the frequency dependence of the imaginary part of the permittivity is shown in Figure 1, *d*. Note the detection of a new (№ 2) rather weak DS feature located at 15 kHz at the temperature of $T = 60$ °C. This feature „drowns" in the № 1 maximum running into it as temperature increases.

Figure 1, *c* shows the Cole-Cole diagrams, that is, the function $\varepsilon''(\varepsilon')$, in the frequency region corresponding to the location of the feature № 1. They are distorted half-circles whose appearance depends weakly on temperature over the entire temperature range used. Thus the „height" of the half-circle $\varepsilon'' = 0.85$ is smaller than its „radius" $[\varepsilon'(f = 0) - \varepsilon''(f = \infty)]/2 = 1.2$.

Figure 1, *e* demonstrates the course of the heated branches of the two DS singularities. The temperature hysteresis loop of the frequency position $f_{\max 1}(T)$ of the maximum $\varepsilon''(f)$ (№ 1) is plotted in Figure 1,*f*. Its „center of gravity" is located at a temperature $T_c = 75$ °C.

3.2. Sample VO_2:Cr(3 %)

The following DS singularities of VO_2:Cr(3 %) sample are observed in the experiment. Two maxima № 1 and № 2 of the $\varepsilon''(f)$ dependence are observed for the imaginary $\varepsilon''(f)$ part of the permittivity (Figure 2, *a*). They are located close to each other at frequencies of $f_{\max} = 10^3 - 10^4$ Hz at the temperature of $T = 55$ °C. The frequencies of maxima move apart as the temperature increases, and the frequency at which the maximum № 2 is located monotonically increases from 10^4 Hz to 0.9 MHz in the temperature interval of 55–65 °C, and this maximum sharply shifts towards high frequencies in the temperature range of 65–80 °C (curves *4, 6* of Figure 2, *b*), so that it is located already at 8 MHz at the temperature of 80 °C. The frequency position of the maximum № 1 does not change much with temperature.

The frequency dependence of the real $\varepsilon'(f)$ part of the dielectric permittivity shows two steps (№ 1 and № 2) located with their middle part in the frequency region $f = 10^3 - 10^6$ Hz (Figure 2, *b*). While the step № 2 is barely „noticeable" at $T = 55$ °C, it can be seen quite clearly at $T = 80$ °C (Figure 2, *b*). As the temperature increases, both steps shift toward higher frequencies, but the № 1 step shifts only slightly, whereas the № 2 step shifts very strongly. So the frequency of the step № 2 sharply increases from 10 kHz to 5 MHz as the temperature increases from 60 to 80 °C. The temperature transformation of the DS of VO_2:Cr(3 %) sample can be traced more definitely, as in the previous case, by taking the frequency derivatives of the DS. The result of differentiating the frequency dependence of the imaginary part of the permittivity is shown in Figure 2, *d*. Also noteworthy here is the clearer identification of rather weak but quite distinguishable DS singularities correlating with maxima 1, 2 (Figure 2, *a*).

The Cole-Cole diagrams $\varepsilon''(\varepsilon')$ have the shape of distorted half-circles (Figure 2, *c*). It can be clearly seen that a second half-circle appears at $T = 60\,^{\circ}\mathrm{C}$, which becomes pronounced at $T = 80\,^{\circ}\mathrm{C}$. The shape of the half-circles weakly depends on temperature, with the „height" of the half-circles at any temperature in the range used being smaller than their „radii".

Figure 2, *e* shows the heating branches of the frequency position hysteresis loop of the two DS singularities. The temperature hysteresis loop of the frequency position of the $f_{\max 2}(T)$ high-frequency maximum $\varepsilon''(f)$ is plotted in Figure 2, *f*. „Center of gravity" of this loop is at temperature $T_c = 67\,^{\circ}\mathrm{C}$.

4. Results of DS calculations

The experimentally measured curves indicate the presence of two singularities (two maxima ε'' and two steps ε') in the DS, as shown in Figures 1, 2. Therefore, they are described on the basis of the presence of two types of relaxants with characteristic times τ_1 and τ_2 in the sample. The dielectric permittivity ε^* has, the following form in this case [8]:

$$\varepsilon^*(\omega) = \varepsilon_\infty + \frac{\Delta\varepsilon_1}{1 + (i\omega\tau_1)} + \frac{\Delta\varepsilon_2}{1 + (i\omega\tau_2)}, \qquad (1)$$

Where $\omega = 2\pi f$ is the angular frequency.

As an example, Figure 3 shows the results of the DS calculation for the sample of VO_2:Cr(3 %). The solid curves of the graphs of the functions $\varepsilon'(f)$ and $\varepsilon''(f)$, as well as the corresponding Cole-Cole diagram, are plotted using the formula (1). The parameters of the Debye (1) formula are chosen so that the calculated curves correspond to the experimental curves obtained at $T = 60\,^{\circ}\mathrm{C}$ (*a*) and $80\,^{\circ}$ (*b*) (before and after semiconductor-metal PT). The provided results indicate that Debye's description qualitatively explains the appearance of the DS. A detailed comparison of the calculation with experiment shows, however, that the maxima and steps in the experimental curves are wider than in the calculated curves, and the experimental CC diagrams do not consititute regular half-circles.

A certain discrepancy between the experimental and calculated data is naturally caused, in our opinion, by the fact that the real sample contains a set of individual relaxants with different but close to each other relaxation times with numerical values distributed in narrow limits near the value of the relaxation time of each type of relaxant. In other words, there is a distribution of numerical values of the relaxation times within a narrow range of variation of the time distribution density. At the same time, several different types of relaxers should appear on the experiment as several maxima of the $\varepsilon''(f)$ function, several steps of the $\varepsilon'(f)$ function, and several half-circles on the CC diagram, of different shapes and widths. That is, the presence of a set of distinct relaxants with close relaxation times will manifest itself for each type of relaxant both as a distortion of the shape of the curves $\varepsilon'(f)$, $\varepsilon''(f)$, and the shape of the semicircles on the CC diagram. This kind of distortions is taken into account by a specially developed analysis method presented in the literature [10,11] in which, according to the expression:

$$\varepsilon^*(\omega) = \varepsilon_\infty + (\varepsilon_s - \varepsilon_\infty) \int_0^\infty \frac{G(\tau)}{1 + i\omega\tau}\, d\tau \qquad (2)$$

function $G(\tau)$ of the distribution of the temporal density of relaxants over relaxation times for each type of relaxant is introduced into consideration. In such a refining Debye description, the Havriliak-Negami (HN) function, for example, is used in the calculations [9]. The parameters of the HN function reflect, as is known, the averaged position of the values of the relaxation times on the time scale (τ_{HN}), as well as the degree of scatter (α_{HN}) and heterogeneity (β_{HN}) of the distribution of relaxation times.

It is possible to achieve a better agreement between the results of the DS calculation and their measurements by varying the parameters of the HN function. DS „corrected" by the HN function by the formula (2) for better matching the experiment (dashed curves), are shown In Figure 3, as an example, along with the DC calculated by the formula (1) (solid curves). It can be seen that the step $\varepsilon'(f)$ „of the non-Debye" DS is wider, the maximum $\varepsilon''(f)$ is smaller, and the shape of the half-circle $\varepsilon''(\varepsilon')$ is distorted. Thus, after a good agreement of the results of the calculation by formula (2) with the data of dielectric measurements has been achieved as a result of fitting, it is possible to judge the shape of the function $G(\tau)$ of the distribution of relaxants over relaxation times from the values of these parameters (see the caption to Figure 3).

5. Discussion of the results obtained

We believe that the frequency position of the maxima $\varepsilon''(f)$, the steps $\varepsilon'(f)$, and the shape of the semicircles in the Cole-Cole diagrams in our samples are physically determined by the characteristics of the particular type of relaxants, namely the relaxation time of the array of free electrons. The characteristic relaxation times in this interpretation are the Maxwell relaxation times $\tau_{\mathrm{M}} = \varepsilon\varepsilon_0/\sigma$ [12], where σ — is the specific electrical conductivity of the crystalline substance. That is, the frequency f of the position of DS singularities is directly proportional to the specific electrical conductivity σ in view of the inversely proportional dependence of the frequency on the Maxwell relaxation time $f = 1/\tau_{\mathrm{M}}$.

The continuous shift of DS singularities to the high-frequency region with increasing temperature in the interval $T = 55{-}60\,^{\circ}\mathrm{C}$ is caused in the proposed model by an increase in the rate of thermal generation of free electrons, i. e., it is associated with an increase in the electrical conductivity of the semiconductor, and, as a consequence,

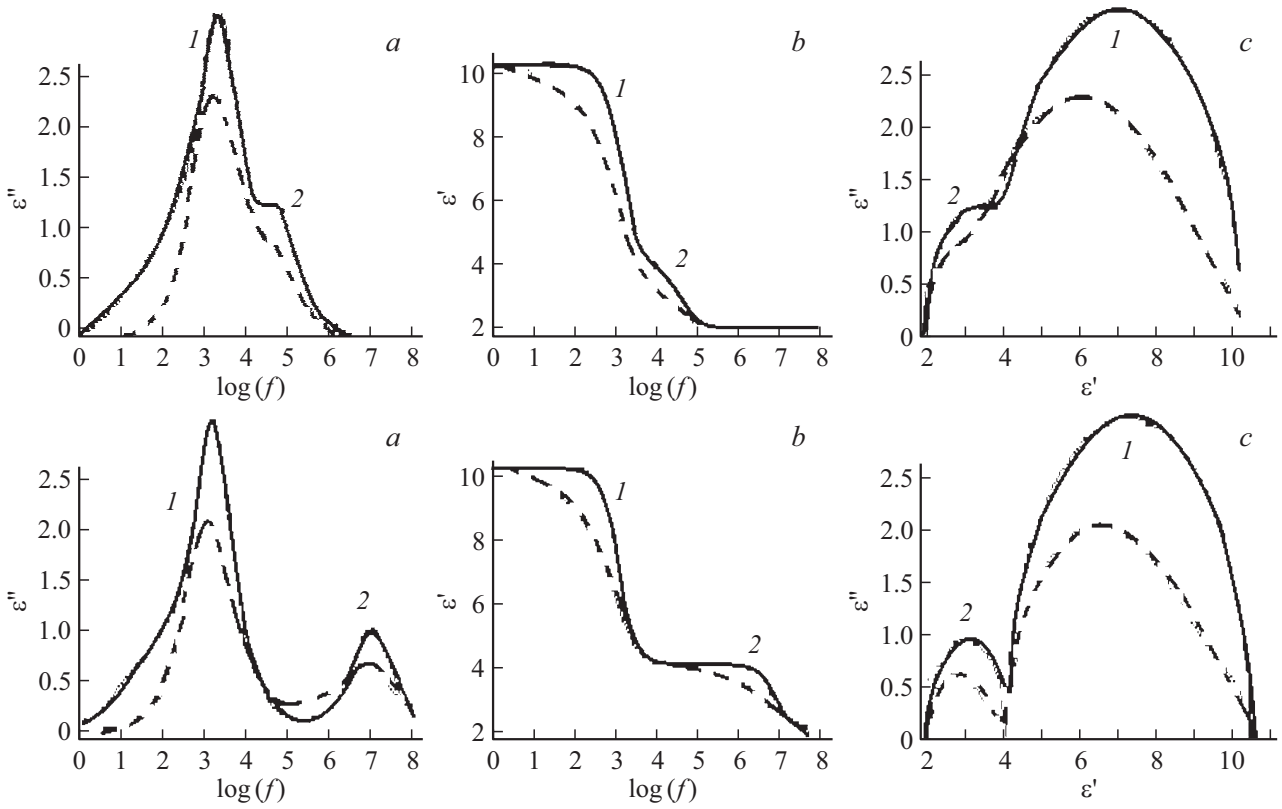

Figure 3. Results of DS calculations for VO_2:Cr(3 %) sample: *a* — at $T = 60\,^{\circ}C$ (below the semiconductor-metal PT temperature), *b* — at $T = 80\,^{\circ}C$ (above the semiconductor-metal PT temperature). $\varepsilon_\infty = 2$, $\Delta\varepsilon_1 = 6.2$, $\Delta\varepsilon_2 = 2$. Solid curves — calculations by formula (1), dashed curves — calculations by formula (2). $(G\tau)$ — Havriliak-Negami function [9] with parameters: $\tau_{HN1} = 10.6 \cdot 10^{-5}$ s, $\alpha_{HN1} = 0.9$, $\beta_{HN1} = 0.9$, $\tau_{HN2} = 4 \cdot 10^{-6}$ s, $\alpha_{HN2} = 0.9$, $\beta_{HN2} = 0.9$ (*a*) and $\tau_{HN1} = 10.6 \cdot 10^{-5}$ s, $\alpha_{HN1} = 0.9$, $\beta_{HN1} = 0.9$, $\tau_{HN2} = 1.6 \cdot 10^{-8}$ s, $\alpha_{HN2} = 0.9$, $\beta_{HN2} = 0.9$ (*b*).

with a decrease in the Maxwell relaxation time. The accelerated thermal shift of DS singularities toward high frequencies in the $T = 60-70\,^{\circ}C$ region is due to the semiconductor-metal phase transition (TP), which results in the metallic conductivity of the material. It should be noted that the specific electrical conductivity σ increases by about three orders of magnitude in this case.

The presence of two distinctive types of DS singularities is attributable to the fact that the polycrystalline vanadium dioxide film consists of three types of grains: strongly and weakly chromium-doped grains, and undoped grains. The nanocrystalline film grains perform a semiconductor-to-metal phase transition (PT) as indicated. It occurs at temperature of $T_c = 75\,^{\circ}C$ in weakly doped (Cr 1 %) grains, which is higher than the PT temperature of undoped grains of VO_2 ($T_c = 67\,^{\circ}C$). For heavily doped grains (Cr 3 %), the PT is not recorded at all in the frequency and temperature intervals of the dielectric spectrometer parameters available for this experiment.

5.1. Macroscopic analysis of experimental results

First of all, we would like to note that the samples of VO_2:Cr(1 %) and VO_2:Cr(3 %) films are different samples synthesized independently. In the synthesis process of the doped sample, metallic Cr particles, falling onto a mica substrate heated to 750 K and migrating on the substrate, form V-Cr and Cr-Cr pairs, which play the role of effective nucleation centers. Therefore, it should be kept in mind that at a small concentration of Cr particles, crystal grains with V-V-V and V-Cr-dimers, which are less fragile than Cr-Cr-dimers, are formed during the synthesis process. The V-V-V and V-Cr-dimers determine the frequency position and temperature behavior of the № 2 maximum (Figure 1, *a*). The stronger Cr-Cr-dimers provide the dominant DS dielectric response of grains with low resonance frequency — maximum № 1 (Figures 1, *a*, 2, *a*) over the response of grains with weak V-V-V-dimers and higher response frequency — a maximum № 2 (Figure 2, *a*).

Thus, phenomenological analysis of the experimental DS and the data in Table 1 reveals the following patterns. Increase of degree of doping with chromium Cr(1 %) → Cr(3 %):

– reduces frequencies of DS singularities: $f_{max\,1} = 1.3 \cdot 10^3$ Hz $< f_{max\,2} = 10^3$ Hz and $f_{max\,1} = 10^3$ Hz $< f_{max\,2} = 10^4$ Hz in films. VO_2:Cr(1 %) and VO_2:Cr(3 %) respectively.

– increases the temperature of the PT: $T_{c1} = 75\,^{\circ}C$ and $T_{c2} = 67\,^{\circ}C$ for VO_2:Cr (1 %) and VO_2 films, respectively.

Table 1. The feature parameters of the frequency derivative function $\varepsilon''(f)$ for the VO_2:Cr film sample with the increase of Cr doping degree

	№	Intensity $\varepsilon''_{\max}$	Frequency $f_{\min}$, Hz	Frequency $f_{\max}$, Hz	T_c, °C	$\Delta[\mathrm{Log}(f)]$
VO_2:Cr(1 %)	1	0.85	$1.3 \cdot 10^3$ (60 °C)	10^6 (100 °C)	75	3
	2	0.2	$1.5 \cdot 10^3$ (60 °C)	–	67	3
VO_2:Cr(3 %)	1	2.2	10^3 (60 °C)	$1.3 \cdot 10^3$ (80 °C)	–	–
	2	0.5	10^4 (60 °C)	–	67	3

Let's look at these items in more detail.

1. When the film grains are doped with chromium ions at low concentration, stronger V-V-V-dimers appear instead of the usual V-V-V-dimers, and even stronger Cr-Cr-dimers appear at high chromium ion concentration. As a consequence, the thermodynamic equilibrium shifts towards lowering the concentration of free electrons in the conduction band, and the specific conductivity of the doped crystal grain decreases. This causes the frequency positions of the DS singularities, determined by the Maxwell relaxation time, to shift to the low-frequency region compared to their frequency positions for undoped grains (Table 1).

2. The increase of the PT temperature of DS singularities is also determined by the formation of high-strength Cr-Cr-dimers when the grains are doped with chromium ions. The point is that due to the shifted thermodynamic equilibrium, the grain specific conductivity values corresponding to doped films will be reached at a higher sample temperature. Therefore, both the heating and cooling branches of the thermal hysteresis loop of the frequency position of the DS singularities are shifted toward higher temperatures. Thus, in the absence of doping, the equilibrium temperature of the semiconductor and metal phases (the semiconductor-metal PT temperature) $t_c = 67$ °C. Weak doping with chromium with the formation of Cr-Cr-dimers increases the phase equilibrium temperature to 75 °C, which corresponds to the new equilibrium temperature of semiconductor and metal phases and coincides with the temperature of the middle of the thermal hysteresis loop at the loop width 10 °C (Figure 1,*f*). Strong doping of the VO_2 film with Cr dopant at a concentration of 3 % shifts the position of the maximum № 1 to the low-frequency region (cf. Figure 1, *a* and Figure 2, *a*) and at the same time excludes the possibility of observing the PT in the temperature range used in the experiment: as the temperature increases to 80 °C, the frequency position of the maximum № 1 practically does not change (Figure 2, *a*). It should be noted that the above results are in good agreement with the study in Ref. [13]. The middle of the thermal hysteresis loop also shifts in this study when Cr is doped toward higher temperatures.

5.2. Microscopic analysis of experimental results

Macroscopic analysis of the data in Table 1 revealed the phenomenological patterns above. A microscopic quantum mechanical explanation of the observed phenomena can also be given on the basis of a comprehensive analysis of the experimental results using the valence bond method and the method of linear combination of atomic orbitals.

The electronic configuration of the chemical elements used in the synthesis of the VO_2:Cr film is given in Table 2. It should be noted that the dopant in Cr doping replaces the V^{4+} ion at the center of the oxygen octahedron and therefore has a valence of +4 in contrast to the typical valence of chromium ions in most molecular compounds of +3.

The orbitals involved in the formation of the oxygen octahedron of the crystal lattice are given in square brackets in Table 2. Orbitals not participating in such formation is provided outside square brackets. They ensure both the integrity of V-V, V-Cr and Cr-Cr-dimers of the semiconductor phase, and the formation of $3d_{\mathrm{bott}} - \pi^*$ energy gap in the electronic spectrum, which plays the role of the band gap of the semiconductor.

Figure 4 shows below the schemes of atomic orbitals ensuring the formation of three types of dimers of semiconductor phase of VO_2 and VO_2:Cr: V-V-dimers, V-Cr-dimers, and Cr-Cr-dimers.

Microscopic analysis of the above schemes leads to the following conclusions.

The V-V-dimers are formed in the semiconductor phase of the undoped VO_2 film sample according to a single principle due to the overlap of the orbitals of the V^{4+} ions not participating in hybridization $3d_{x2-y2}$ located in the base centers of adjacent oxygen octahedrons (Figure 4, *a*). However, the degree of overlap of $3d_{xz}$ and $3d_{yz}$ orbitals with $2p_z$-orbitals of oxygen ions in the vertices of oxygen octahedrons (which ensures a gap between the energies of π-orbitals and antibinding π^*-orbitals and, accordingly, the energy gap $d_{\mathrm{bott}} - \pi^*$, i.e., the width of the band gap [14]) should depend both on the external Laplace pressure of the nanocrystallite surface and on the adhesive mechanical stress during the interaction of the nanocrystallite with the substrate. Both of these factors determine the temperature T_c of the phase equilibrium that is equal to 67 °C [2].

The situation is somewhat more complicated in the semiconductor phase of the VO_2 film sample doped with Cr with a concentration of 1–3 %: the film synthesized on the substrate surface consists of grains with different contents of all three types of dimers.

Weak doping (less than 0.5 %) occurs in some fraction of the total number of nanocrystallites whose surface

Table 2. Electron configuration of ions V^{4+}, Cr^{4+} and O^{2-}

$\mathbf{VO}_x$	$\mathbf{V^{4+}}$	[Ar] $3d^0_{yz}(1)$ $3d^0_{xz}(1)$ $[\mathbf{3}d^1_{z2}(\mathbf{1})\mathbf{3}d^1_{xy}(\mathbf{1})\mathbf{4}s^2(\mathbf{1})\mathbf{4}p^0_x(\mathbf{1})\mathbf{4}p^0_y(\mathbf{1})\mathbf{4}p^0_z(\mathbf{1})]$ $\mathbf{3}d^1_{x2-y2}(\mathbf{1})$
$\mathbf{X = 2}$	$\mathbf{Cr^{4+}}$	[Ar] $\mathbf{4}p^0_z(\mathbf{1})$ $[\mathbf{3}d^1_{z2}(\mathbf{1})\mathbf{3}d^1_{xy}(\mathbf{1})\mathbf{3}d^0_{xz}(\mathbf{1})\mathbf{4}s^2(\mathbf{1})\mathbf{4}p^0_x(\mathbf{1})\mathbf{4}p^0_y(\mathbf{1})]$ $\mathbf{3}d^1_{yz}(\mathbf{1})\mathbf{3}d^1_{x2-y2}(\mathbf{1})$
	$\mathbf{O^{2-}}$	$1s^2(1)$ $\mathbf{2}p^2_z(\mathbf{1})$ $[2s^2(1)2p^1_x(1)2p^1_y(1)]$

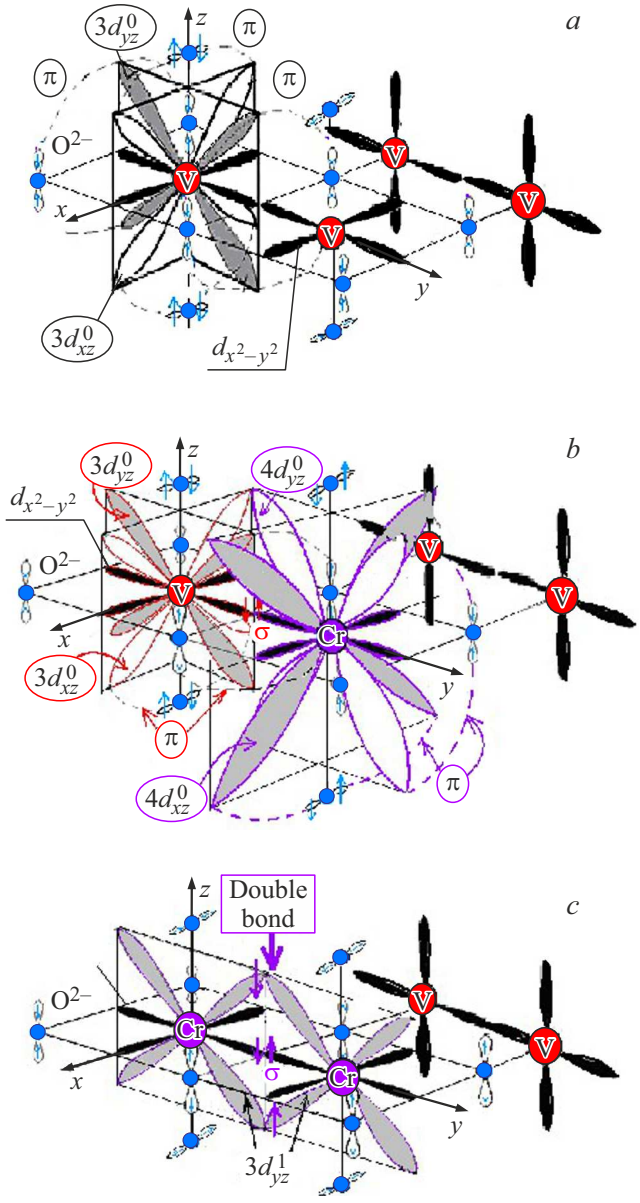

Figure 4. *a* — V-V-dimers of undoped VO_2 film; *b* — V-Cr-dimers; *c* — Cr-Cr-dimers of weakly and heavily doped VO_2 film.

curvature limits the access of the doping impurity into the crystallite thickness. Weak doping in principle lowers the PT temperature, although only slightly [15,16]. The reason for the decrease of the temperature T_c is that V-Cr-type dimers are formed along with V-V-V-dimers in case of weak doping with Cr dopant, the properties of which are radically different from the properties of V-V-V and Cr-Cr-dimers. The situation is clarified by Figure 4, *b*. It shows that one of the two additional Cr electrons compared to the V atom is forced into the π^*-zone, which in this case is also modified from the typical one and is created by the overlap of the $4d_{xz}$ orbitals and $4d_{yz}$ orbitals with the p_z-orbital of the oxygen ion, rather than by the overlap of $3d_{xz}$ orbitals and $3d_{yz}$ orbitals with the p_z-orbital of oxygen. This overlap turns out to be much smaller due to the much larger difference in the geometric sizes of the overlapping orbitals at the drop-shape of their branches. This leads, according to the theory of linear combination of atomic orbitals, to a narrowing of the energy gap $d_{\text{bott}} - \pi^*$, which together with the additional occupancy of the π^* conduction band by an electron from the $4s^1$-orbital lowers T_c.

VO_2 nanocrystallites whose cross-section exceeds a critical value that prevents, through the action of Laplace pressure, the introduction of chromium ions into the nanocrystallite during synthesis, i.e., those that allow full Cr doping contain Cr-Cr-dimers of increased strength together with h V-V and V-Cr-dimers (Figure 4, *c*). The high strength of Cr-Cr-dimers is attributable to their double chemical bonds: σ-bonds between $3d_{x2-y2}$-orbitals and simultaneously σ-bonds between $3d_{yz}$-orbitals of neighboring octahedrons, which in Cr atom have an additional electron providing π-bonding in contrast to V-V-V-dimers. It is Cr-Cr-dimers in small concentrations that cause the increase of the critical PT temperature to 75 °C for weakly doped grains (1 %) and the absence of the possibility to register the occurrence of PT in the temperature region (60–80) °C for samples with a high content of the chromium impurity (3 %).

6. Conclusion

It is shown that dielectric spectroscopy allows to effectively control the singularities of the dielectric response of a thin-film nanocrystalline system, including the parameters of relaxation processes occurring in it. At the same time, dielectric spectroscopy provides selective control of numerical values of physical parameters of different-sized groups of nanocrystals randomly mixed on the substrate surface during synthesis.

It is found that two singularities are observed in the DS of undoped and doped VO_2 nanocrystalline films doped with different Cr concentrations, the intensities of which are very different from each other for different doping degrees (Table 1). It is shown that the leading intensity feature of the DS spectrum changes during the transition from weak

to strong doping degree. For VO_2:Cr(1 %), the leading impurity is the first feature on the low-frequency side of the spectrum with a maximum № 1 at frequency 1.3 at 60 °C kHz and a shift in the position of this maximum to 1 MHz when the sample is heated to 100 °C; at high concentration of Cr(3 %) ions, the leading feature is the spectrum with a more intense maximum № 1 located at the frequency of 1 kHz at 60 °C, with no thermal frequency shift up to 100 °C.

It is shown that, despite the high degree of doping of VO_2Cr(3 %), a strong thermal frequency shift is found not at the strong intensity but at the weak intensity maximum № 2 (from a frequency value of 10 kHz at 60 °C to a value of 8 MHz at 80 °C). This fact suggests the presence of a small amount of undoped VO_2 grains in the heavily Cr ion-doped VO_2 film.

It is found that an increase in the degree of chromium doping from Cr(1 %) to Cr(3 %) is accompanied by:

a) A decrease of the frequency of DS singularities: $f_{\max 1} = 10^3$ Hz $< f_{\max 2} = 1.3 \cdot 10^3$ Hz, which takes place in VO_2 films, and also $f_{\max 1} = 10^3$ Hz $< f_{\max 2} = 10^4$ Hz, which takes place in VO_2:Cr (1 %) and VO_2:Cr (3 %) films, respectively;

b) By increasing the temperature of the PT: $T_{c1} = 75$ °C compared to $T_{c2} = 67$ °C for VO_2:Cr(1 %) and undoped VO_2 films, respectively;

c) The change of the dominant intensity of the DS feature (the change of the maximum № 1, the frequency position of which depends on temperature for the weakly doped film, to a more intense maximum № 1, the frequency position of which does not depend on temperature for the heavily doped film).

It is found that the Debye calculations of the DS of the thin film sample of VO_2:Cr qualitatively coincide with the experimental results. A better agreement between the calculation results and the measurements is obtained by involving the Havriljak-Negami function as a function of the distribution of relaxants by relaxation times.

The specific type of relaxers that determines the relaxation process of the dielectric response is identified and it is shown that the relaxation time of the response is determined by the relaxation time of the free electron array. The characteristic relaxation times are the Maxwell relaxation times $\tau_{\text{M}} = \varepsilon\varepsilon_0/\sigma$ [12], where σ — the specific electrical conductivity of the crystalline substance.

It has been found that the continuous shift of DS singularities to the high-frequency region with increasing temperature in the interval $T = 20-60$ °C is associated with an increase in the rate of thermal generation of free electrons, i. e., with an increase in the electrical conductivity of the semiconductor, and, as a consequence, with a decrease in the Maxwell relaxation time. The accelerated temperature shift of the DS singularities towards high frequencies is due to the semiconductor-metal PT, in which the metallic conductivity of the material appears, significantly reducing the Maxwell relaxation time.

It is shown that the presence of several types of DS singularities is due to the fact that the polycrystalline vanadium dioxide film consists of several types of grains: heavily doped, weakly chromium-doped, and undoped. For strongly doped grains, the PT in the operating frequency and temperature range of the dielectric spectrometer is not registered, going beyond the measurement limits, whereas in case of weakly doped grains the PT takes place at elevated temperature ($T_c = 75$ °C) compared to the PT temperature in the film with undoped grains of VO_2 ($T_c = 67$ °C).

The decrease in the frequencies of all DS singularities as the degree of chromium doping increases is explained, which is due to the following within the proposed model. Namely, the central point of the model is the correspondence of the lowest-frequency maxima of DS (№ 1) to the highest PT temperature (T_c). At the same time, it appears that doping of the VO_2 film with Cr dopant not only lowers the partial position of these DS maxima due to the decrease in the electrical conductivity of the material, but also simultaneously increases the T_c of the phase transition.

A microscopic analysis of the experimental results was carried out, which showed that V-V-dimers are formed in the semiconductor phase of the undoped sample of VO_2 film according to a single principle due to the overlap of $3d^1_{x2-y2}$ orbitals of V^{4+} ions not participating in hybridization, located in the base centers of neighboring oxygen octahedrons (Table. 2). V-Cr-dimers are also formed in the semiconductor phase of a sample weakly doped with Cr with a chromium concentration of about 1 %, due to the overlap of $3d^1_{x2-y2}$-orbitals of vanadium and chromium ions carrying one electron each. At the same time, the $3d^1_{yz}$ orbital of the chromium ion not involved in hybridization although it contains one electron, cannot form a π-bond with a similar orbital of the vanadium ion, since the vanadium ion has an empty $3d^0_{yz}$ orbital. Therefore, the electron from the $3d^1_{yz}$ orbital of the chromium ion goes to the conduction band, lowering T_c. At the same time, Cr-Cr-dimers with a double bond which could be formed by the overlap of $3d^1_{x2-y2}$ and $3d^1_{yz}$ orbitals of adjacent chromium ions, practically are not formed due to the high spatial distance of chromium ions from each other at a low degree of doping. Obviously, almost every ion Cr^{4+} neighbors only on ion V^{4+} in case of low doping degree. Weak doping is formed in some fraction of the total number of nanocrystallites in which the high surface curvature limits the access of the doping impurity into the crystallite. Thus, weak doping during the formation of V-Cr-dimers in principle lowers the PT temperature, although insignificantly. In the case of a more heavily Cr-doped film sample with a chromium concentration slightly greater than 0.5 % not only dimers intrinsic to the undoped material V-V-dimers are present in its semiconductor phase of VO_2, but also dimers corresponding to both the weakly doped and heavily doped material: V-Cr-dimers and Cr-Cr-dimers. It is shown that VO_2 nanocrystallites of such a large size and, consequently, such a small surface curvature that they allow their full Cr doping due to the negligible Laplace pressure of the surface, have Cr-Cr-dimers of enhanced strength. The increased strength of the dimers is attributable

to the presence of a double bond in the Cr-Cr-dimers: π-bonds between $3d^1_{x2-y2}$-orbitals of Cr ions of neighboring octahedra and, in addition, π-bonds between cross-shaped $3d^1_{yz}$-orbitals of Cr ions of neighboring octahedra. These orbitals of the Cr atom have, in contrast to the analogous orbitals of V-V-V-dimers, an additional electron, providing the formation of π-bonds. The result of the presence of the double bond is a significant increase in the critical temperature (T_c) of PT from 67 to 75 °C for weakly doped grains (1 %) and the absence of PT in the temperature region (60−80) °C for grains with high content of chromium doping impurity (3 %), because T_c of highly alloyed samples is beyond the temperature range used in this work.

Funding

The study was partially carried out by an internal grant of the A.I. Hertzen Russian State Pedagogical University (project № 43-VG).

Conflict of interest

The authors declare that they have no conflict of interest.

References

[1] N.F. Mott. Metal–Insulator Transitions. Nauka, M. (1979). Taylor & Francis Ltd, London (1974). 342 p.
[2] A.A. Bugaev, B.P. Zakharchenya, F.A. Chudnovsky. Fazovyj perekhod metall–poluprovodnik i ego primenenie. Nauka, L. (1979). p. 183. (in Russian).
[3] W. Bruckner, H. Opperman, W. Reichelt, G. Wolf, F.A. Chudnovsky, E.I. Terukov. Vanadium dioxide. Academy-Verlag, Berlin (1983).
[4] Modern sensors. Handbook / J. Fryden; translated by Y.A. Zabolotnaya; ed. by E.L. Svintsov. Tekhnosfera, M. (2005). p. 588. (in Russian).
[5] E. Pavlyukovich. Mikrosistemy vysokoskorostnoj pamyati. Vestnik elektroniki (2017). № 3−4. PP. 38–41. (in Russian).
[6] B.E.A. Saleh, M.K. Teich. Optika i fotonika. Principy i primeneniya. Per. s angl.: Uchebnoe posobie. V 2 t. Intellekt, Dolgoprudnyj (2012). p. 1544. (in Russian).
[7] A.V. Ilinskiy, R.A. Kastro, M.E. Pashkevich, E.B. Shadrin. FTP **54**, *4*, 331 (2020).
[8] A.V. Il'inskij, E.B. Shadrin. FTT **66**, *5*, 708 (2024). (in Russian).
[9] A.S. Volkov, G.D. Koposov, R.O. Perfil'ev, A.V. Tyagunin. Optika i spektroskopiya **124**, *2*, 206 (2018). (in Russian).
[10] A.S. Volkov, G.D. Koposov, R.O. Perfilyev. Optika i spektroskopiya **125**, *3*, 364 (2018). (in Russian).
[11] S. Havriliak, S. Negami. J. Polym. Sci. **14**, 99 (1966).
[12] Fizicheskaya entsiklopediya. Bol'shaya Rossijskaya enciklopediya, M. (1992). P. 602.
[13] V.N. Andreev V.A. Klimov, M.E. Kompan, B. Melekh. FTT **56**, *9*, 1795 (2014).
[14] J.B. Goodenough. Czech. J. Phys. B **17**, 304 (1967).
[15] J.B. Goodenough. In: Progress in Inorganic Chemistry / Ed. H. Reiss. Pergamon Press, Oxford **5**, 145 (1971).
[16] X. Wang, E. Suhr, L. Banko, S. Salomon, A. Ludwig. Applied Electronic Materials **4**, p. A-G (2020).

Translated by A.Akhtyamov